Eur. Phys. J. B **16**, 429–434 (2000)

THE EUROPEAN PHYSICAL JOURNAL B

EDP Sciences

Magnetic properties of $ErFe_6Ga_6$ studied by magnetization and neutron diffraction

K. Prokeš[1,a], R.T. Gramsma[2], Y. Janssen[2], E. Brück[2], K.H.J. Buschow[2], and F.R. de Boer[2]

[1] Hahn-Meitner-Institute, SF-2, Glienickerstrasse 100, 141 09 Berlin, Germany
[2] Van der Waals-Zeeman Institute, University of Amsterdam, Valckenierstraat 65, 1018 XE Amsterdam, The Netherlands

Received 24 November 1999 and Received in final form 27 March 2000

Abstract. Neutron-diffraction experiments reveal that $ErFe_6Ga_6$ forms in the tetragonal $ThMn_{12}$-type of structure (space group I_4/mmm). The Fe sublattice orders ferromagnetically below $T_C = 509$ K. The Er moments order antiparallel to the Fe moments which, below about 250 K, leads to a decrease of the total magnetization. The easy magnetization direction of $ErFe_6Ga_6$ is perpendicular to the c-axis in the whole temperature range. Refinement at 2 K shows that $ErFe_6Ga_6$ orders ferrimagnetically with Er moments of 8.5 (2) μ_B and Fe moments at the 8(j) site of 1.9 (1) μ_B and at the 8(f) site of 1.7 (1) μ_B, respectively. At room temperature, $ErFe_6Ga_6$ exhibits the same type of magnetic order, however with substantially lower Er moments of 1.0 (4) μ_B and Fe moments at the 8(f) site of 1.2 (2) μ_B. The Fe moments at the 8(j) site amount to 1.9 (5) μ_B/Fe.

PACS. 75.50.Gg Ferrimagnetics – 75.30.Gw Magnetic anisotropy – 75.25.+z Spin arrangements in magnetically ordered materials (including neutron and spin-polarized electron studies, synchrotron-source x-ray scattering, etc.)

1 Introduction

Pseudobinary rare-earth (R) Fe-rich intermetallic compounds crystallizing in the tetragonal $ThMn_{12}$-type of structure have been the subject of intensive studies over the last decade due to their possible use in technical applications [1]. The otherwise non-existent crystal structure can be stabilized by alloying with a transition and/or non-transition element. The stabilizing element influences also the magnetic properties. This is also the case for rare- earth compounds crystallizing in the $ThMn_{12}$-type of structure stabilized by Ga [2]. Iron-rich $RFe_{12-x}Ga_x$ (R = rare earth) compounds with R = Y or Gd have been studied by Burzo *et al.* [3]. These compounds are reported to be stable only for $1 \leq x \leq 2$. $RFe_{12-x}Ga_x$ compounds comprise both Fe and R moments with ordering temperatures above 400 K [4,5]. For the compounds with the heavy R elements a ferrimagnetic ground state with Fe and R moments antiparallel to each other at low temperatures and ferromagnetic (only significant Fe moments present) at higher temperatures have been reported [5]. In contrast, for compounds with light R and Y, ferromagnetism has been found at all temperatures below T_C [5]. For all $RFe_{12-x}Ga_x$ compounds easy-plane type of magnetic anisotropy was found [5].

In this paper, we report on the magnetic properties of $ErFe_6Ga_6$, studied by magnetization and neutron-diffraction techniques in a wide temperature range.

2 Experimental

Polycrystalline samples of $ErFe_6Ga_6$ have been prepared by arc-melting appropriate amounts of the constituting elements under argon atmosphere in several small batches (∼3–4 g each). They were wrapped in Ta-foil and subsequently annealed for 10 days in vacuum-sealed quartz ampoules at 1000 °C. The purity and composition homogeneity of each batch was checked by means of X-ray diffraction. For comparison, we have also prepared an YFe_6Ga_6 sample, under the same conditions.

X-ray diffraction showed two of the batches of $ErFe_6Ga_6$ to be nearly single phase. The others were found to contain several other phases and they were not used in the present study. However, even in the purest batch some traces of α-Fe have been detected. The YFe_6Ga_6 sample turned out to be single phase having the same structure as $ErFe_6Ga_6$. Magnetization measurements on $ErFe_6Ga_6$ were performed from 5 up to 350 K using a quantum design SQUID magnetometer and from 300 up to 710 K using a home-built Faraday balance.

Neutron-diffraction data at 2, 290 and 547 K were obtained in the multicounter diffractometer E6 at the Hahn-Meitner-Institute using an incident-neutron wavelength of 2.4 Å. To create elevated temperatures, the ILL

[a] e-mail: prokes@hmi.de
On leave from: Department of Electronic Structures, Charles University, 12116 Prague 2, The Czech Republic

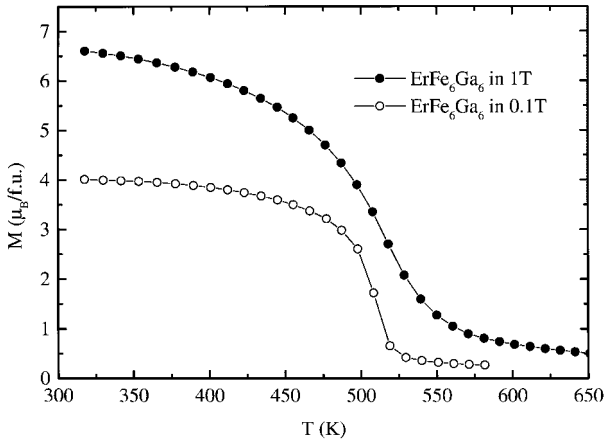

Fig. 1. High-temperature part of the temperature dependence of the magnetization of $ErFe_6Ga_6$ measured in fields of 0.1 and 1 T.

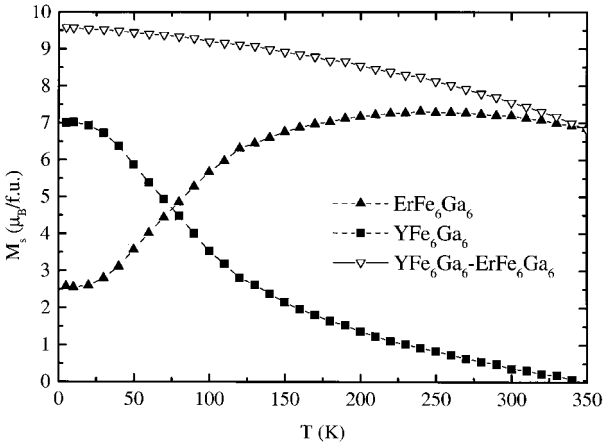

Fig. 2. Temperature dependence of the magnetization of $ErFe_6Ga_6$ determined by fitting the data to an approach to saturation, together with data on YFe_6Ga_6, obtained in the same manner, and the difference between them.

standard orange furnace has been employed. For these measurements about 9 g of $ErFe_6Ga_6$ was ground and encapsulated in a vanadium container. The data were analyzed by means of the Rietveld profile procedure [6] using the program Fullprof [7]. The appropriate neutron-scattering lengths were used [8], $b_{Er} = 0.7790 \times 10^{-12}$ cm, $b_{Fe} = 0.9450 \times 10^{-12}$ cm and $b_{Ga} = 0.7988 \times 10^{-12}$ cm.

3 Results

3.1 Magnetic properties

In Figure 1 the temperature dependence of the magnetization M is shown, as measured in the Faraday balance in applied magnetic fields of 0.1 T and 1 T. As can be seen from the inflection point in the $M(T)$ curve taken at 0.1 T, $ErFe_6Ga_6$ orders magnetically below $T_C = 509$ K. The inflection point shifts towards higher temperatures as the applied field is increased, pointing to ferromagnetic or ferrimagnetic order in $ErFe_6Ga_6$.

The temperature dependence of the spontaneous magnetization M_s measured below 350 K using a SQUID magnetometer on a powder sample oriented along the easy-magnetization direction (the grains were magnetically aligned by a field of 1 T and fixed by epoxy) is shown in Figure 2. Saturation magnetization values M_s were obtained by fitting the data to an approach to saturation curve as described in [9]. M_s increases upon lowering of the temperature, attains a maximum of 7.2 μ_B/f.u. around 250 K and then decreases upon further lowering the temperature to a value of 2.6 μ_B/f.u. The decrease of M_s below 250 K is an indication of ferrimagnetic order in $ErFe_6Ga_6$. In the same picture we also show data on YFe_6Ga_6, obtained under the same conditions. This compound has been reported to order ferromagnetically [5] with a magnetic moment of 1.45 μ_B/Fe. It is observed that the spontaneous magnetization of this sample increases monotonically with decreasing temperature. At the lowest temperature, it saturates at 9.6 μ_B/f.u. Due to the

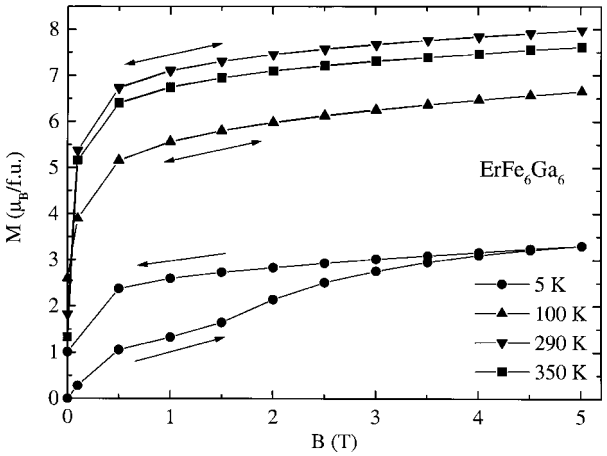

Fig. 3. Field dependence of the magnetization of $ErFe_6Ga_6$ measured at various temperatures on powder fixed with its easy-magnetization axis along the applied field.

fact that Y is non-magnetic, such a value leads to an average moment per Fe atom of 1.6 μ_B. Supposing that Fe has in both systems the same magnetic moment, *i.e.* that the crystal structures are the same including the distribution of atoms (as indicated by X-ray diffraction) and that also effects arising from crystal fields are the same, we can roughly estimate the size of the Er moments in $ErFe_6Ga_6$. This is shown in Figure 2 by subtracting the magnetization of $ErFe_6Ga_6$ from that of YFe_6Ga_6. At 300 K, Er moment amounts to about 0.5 μ_B/f.u. and it increases monotonically with decreasing temperature reaching a calculated value of 7.0 μ_B/Er at 5 K. Let us note that this value has to be taken with caution due to a small presence of α-Fe in $ErFe_6Ga_6$ sample which affects this analysis.

In Figure 3 we show the field dependence of the magnetization measured up to 5 T at several temperatures up to 350 K. The magnetization curves show a slight saturation tendency. However, even around 5 T the susceptibility is still high. At the lowest temperature,

there is a considerable hysteresis between the ascending and descending-field branches which, however, disappears above 30 K. At 5 K, the magnetization reaches a value of 3.3 μ_B/f.u. in 5 T. With increasing temperature, the magnetization curves shift to higher values attaining a maximum around 250 K. Above this temperature, the curves shift to lower values again.

From the above-presented data it follows that $ErFe_6Ga_6$ orders most probably ferrimagnetically with the Er and Fe moments oriented antiparallel to each other. Additionally, X-ray diffraction on magnetically aligned powder has indicated that $ErFe_6Ga_6$ exhibits easy-plane type of magnetic anisotropy (*i.e.* moments are perpendicular to the tetragonal axis).

3.2 Crystal structure

The diffraction pattern recorded above the highest magnetic phase transition at 547 K, *i.e.* in the paramagnetic state of $ErFe_6Ga_6$, shows the characteristics of the body-centered tetragonal $ThMn_{12}$-type of structure with Miller indices satisfying the reflection rule $(h+k+l) = 2n$. Therefore, all refinements were performed with the I_4/mmm space group. The origin of the unit cell was chosen with the Er atoms at the 2(a) (0, 0, 0) sites and with the Fe and Ga atoms distributed over the 8(f) sites at (1/4, 1/4, 1/4), the 8(i) sites at (x, 0, 0) and the 8(j) sites at (x', 1/4, 0). It is well-known for rare-earth intermetallic compounds with the $ThMn_{12}$-type of crystal structure that there is a preferred site occupancy of the stabilizing element (*e.g.* $ErFe_4Al_8$, in which Fe only occupies the 8(f) sites, or $ErCo_{10}Mo_2$, where Mo only occupies the 8(i) sites [10,11]). This preferred occupation over the available sites may have a profound influence on the magnetic properties. Both the Fe and Ga atoms were in the process of refinement initially set free to distribute over the three sites. The neutron scattering lengths of Fe and Ga are not very different. This results in a small contrast and in difficulties to decide which positions are taken by Fe and which by Ga. Nevertheless, it emerged quite clearly that the Fe atoms occupy the 8(f) sites and the Ga atoms occupy the 8(i) positions. The rest of the Fe and Ga atoms are distributed statistically over the 8(j) sites. The measured diffraction profile together with the best fit are shown in Figure 4.

The fit, comprising scale factor, cell parameters, crystallographic-position parameters, background and peak-profile parameters and overall isotropic thermal factor could not, however, account for the strong reflection at $2\theta \approx 72.6°$ and for the two small peaks at 55.4 and 71.1°, denoted in Figure 4 by the symbol "i". In addition to this, we observe a small amount of intensity superimposed on top of the 002 and 202 reflections at $2\theta = 57.4$ and 67.8°. These reflections originate from impurities present in our sample. The strongest secondary-phase reflection at $2\theta \approx 72.6°$ is due to presence of α-Fe (about 4 wt.%), which has been treated as magnetic. This in turn suggests that there is a Fe deficiency in the main phase. However, including the Fe occupation as a free parameter did not improve quality of the fit substantially. Therefore, we conclude that the main phase has nearly an ideal 1:6:6 stoichiometry. This further suggests that the other secondary phases should consist from Er and Ga only. However, we failed to identify them.

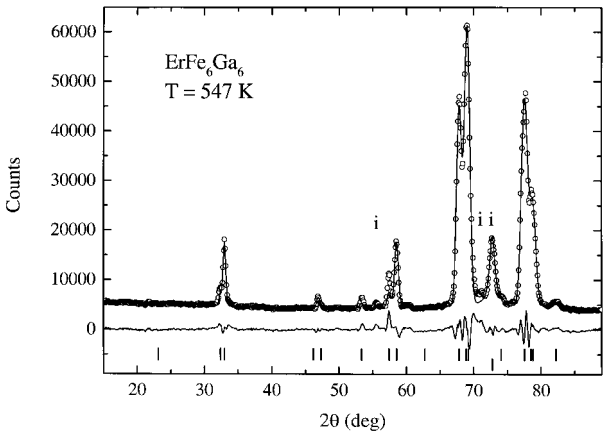

Fig. 4. Neutron-diffraction spectrum of $ErFe_6Ga_6$ recorded in the paramagnetic state at 547 K. The full line through the symbols represents the best fit and the full line at the bottom represents the difference between the experimental data and the fit. The positions of the structural Bragg peaks of α-Fe and $ErFe_6Ga_6$ are marked from the bottom. Impurity peaks are denoted by "i".

Our results concerning the main $ErFe_6Ga_6$ phase are in good agreement with literature values [5] and with our X-ray data refinement. Results of the best fits of both neutron and X-ray data sets keeping occupation number fixed are summarized in Tables 1 and 2, respectively.

3.3 The low-temperature ferrimagnetic structure

As the temperature is lowered, the intensity of some Bragg reflections appears to increase. This is due to magnetic order. Temperature dependencies of integrated intensities of three of the peaks are shown in Figure 5. All reflections can be indexed within the original crystal tructure, *i.e.* the magnetic structure is commensurate with the crystal structure and the propagation vector is equal to $\mathbf{q} = (0, 0, 0)$. This is true in the whole temperature range below T_C down to 2 K, the lowest temperature of the experiment. In the inset of Figure 5 we show several typical diffraction spectra taken between 2 and 540 K.

Magnetic measurements suggests that the Er and Fe moments are coupled antiparallel to each other. Initial refinements with the angle between magnetic moments and the tetragonal axis set as free parameter supported this idea. Therefore, in the next steps we kept this condition throughout the refinement. It is also well-known that, in tetragonal crystal structures, that are highly symmetric, it is not possible to refine the angle that the magnetic moments make within the plane. However, it is possible to refine the angle υ with the tetragonal axis [12]. We have performed a series of refinements changing the angle with the tetragonal axis and keeping the Er and Fe moments antiparallel. The results of this procedure are summarized

Table 1. Structural parameters of $ErFe_6Ga_6$ determined above the magnetic phase transition (in paramagnetic state) at 547 K using neutron diffraction.

Space group:		I_4/mmm	Neutrons $T = 547$ K (paramagnetic)
Atom	Site	Pos. parameters	Occupation
Er	2(a)	000	1.00 (f)
Fe	8(f)	1/4, 1/4, 1/4	1.00 (f)
Fe	8(j)	0.2798 (9), 1/2, 0	0.50 (f)
Ga	8(j)	0.2798 (9), 1/2, 0	0.50 (f)
Ga	8(i)	0.3414 (9), 0, 0	1.00 (f)
$B_{ov} = 0.9$ (1) Å^2			
Lattice parameters:	$a = 859.598$ (188) pm		$c = 508.170$ (107) pm
R factors:	$R_p = 4.78\%$	$R_{wp} = 6.32\%$	$R_B = 2.52\%$

Table 2. Structural parameters of $ErFe_6Ga_6$ determined at room temperature by means of X-ray diffraction.

Space group:		I_4/mmm	X-ray $T = 290$ K (paramagnetic)
Atom	Site	Pos. parameters	Occupation
Er	2(a)	000	1.00 (f)
Fe	8(f)	1/4, 1/4, 1/4	1.00 (f)
Fe	8(j)	0.2833 (11), 1/2, 0	0.50 (f)
Ga	8(j)	0.2833 (11), 1/2, 0	0.50 (f)
Ga	8(i)	0.3349 (9), 0, 0	1.00 (f)
$B_{ov} = 0.4$ (1) Å^2			
Lattice parameters:	$a = 858.021$ (79) pm		$c = 505.939$ (86) pm
R factors:	$R_p = 6.1\%$	$R_{wp} = 8.0\%$	$R_B = 5.1\%$

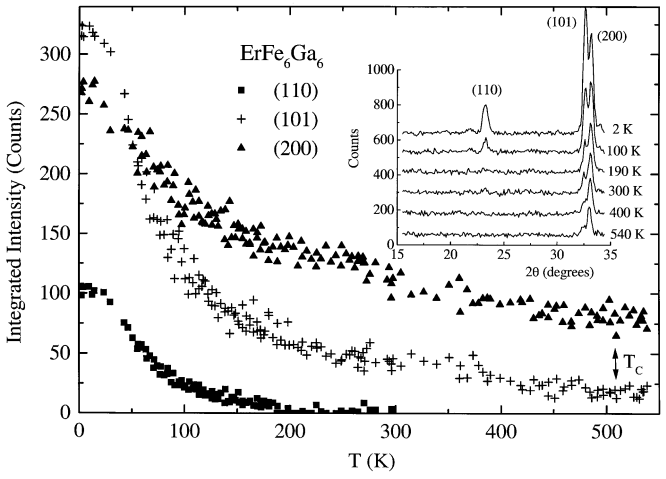

Fig. 5. The temperature dependence of three reflections determined by integration of individual peaks. Note the similarity with the "YFe_6Ga_6-$ErFe_6Ga_6$" curve in Figure 3. In the inset several representative diffraction spectra taken at various temperatures are shown.

in the inset of Figure 6. The fitting also included, in addition to the paramagnetic-state phase refinement, magnetic moments on the Er and the Fe atoms. The best fit led to a collinear magnetic structure with the moments oriented perpendicular to the tetragonal axis. The refined magnetic moments are $\mu_{Er} = 8.5$ (2) μ_B, $\mu_{Fe}8(j) = 1.9$ (1) μ_B and $\mu_{Fe}8(f) = 1.7$ (1) μ_B. The measured diffraction profile together with the best fit and the difference between them are shown in Figure 6. The numerical results are summarized in Table 3. It can be seen that, in addition to impurity reflections mentioned in the preceding paragraph, there are some other low-intensity reflections that originate, most probably, from the magnetic ordering of impurity phases, because we were unable to index them in a systematic way using a second propagation vector. The good agreement between the measured and calculated spectra gives us confidence that the distribution of the Fe and Ga atoms over the 8(f), 8(i) and 8(j) positions is correct. This conclusion is clearly possible thanks to the fact that only the Fe atoms are magnetic.

3.4 The intermediate-temperature magnetic structure

We have also collected data at room temperature ($T =$ 290 K) in order to determine the magnetic structure in the temperature range with the highest magnetization values (see Fig. 2). Inspection of the Bragg reflections reveals that also at this temperature the propagation vector equals $\mathbf{q} = (0, 0, 0)$, as at low temperature. However, some reflections that were present at low temperature are hardly visible at room temperature. We have performed a similar series of fits changing the angle between the moments and

Table 3. Crystallographic and magnetic-structure parameters of $ErFe_6Ga_6$ determined at 2 K.

Space group:		I_4/mmm	Neutrons $T = 2$ K (ferrimagnetic)	
Atom	Site	Pos. parameters	Occupation	Moment
Er	2(a)	000	1.00 (f)	8.52 (15)
Fe	8(f)	1/4, 1/4, 1/4	1.00 (f)	1.74 (8)
Fe	8(j)	0.2730 (14), 1/2, 0	0.50 (f)	1.94 (9)
Ga	8(j)	0.2730 (14), 1/2, 0	0.50 (f)	0
Ga	8(i)	0.3372 (12), 0, 0	1.00 (f)	0
$B_{ov} = 0.2$ (1) Å^2				
Lattice parameters:		$a = 855.496$ (72) pm	$c = 504.498$ (54) pm	
R factors:	$R_p = 5.94\%$	$R_{wp} = 7.96\%$	$R_B = 1.42\%$	$R_M = 2.11\%$

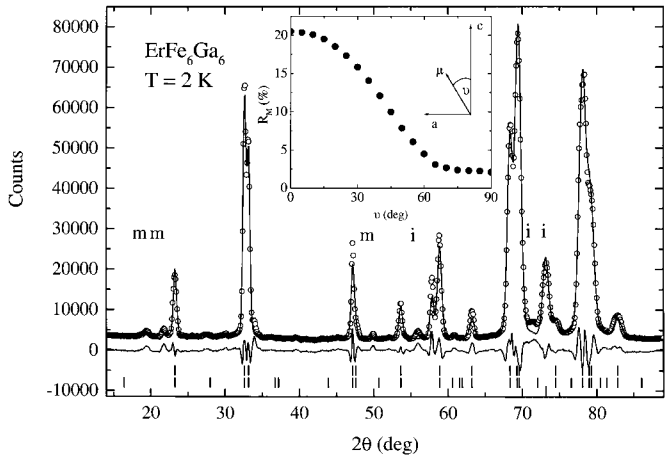

Fig. 6. Neutron-diffraction spectrum of $ErFe_6Ga_6$ recorded in the ferrimagnetic state at 2 K. The full line through the symbols represents the best fit and the full line at the bottom represents the difference between the experimental data and the fit. The positions of α-Fe Bragg peaks and the magnetic and structural Bragg reflections of $ErFe_6Ga_6$ are marked in the first, second and the third row from the bottom. In the inset, the quality-of-fit factor is shown as a function of the angle between the tetragonal axis and magnetic moments. Structural and magnetic impurity peaks are denoted by "i" and "m" respectively.

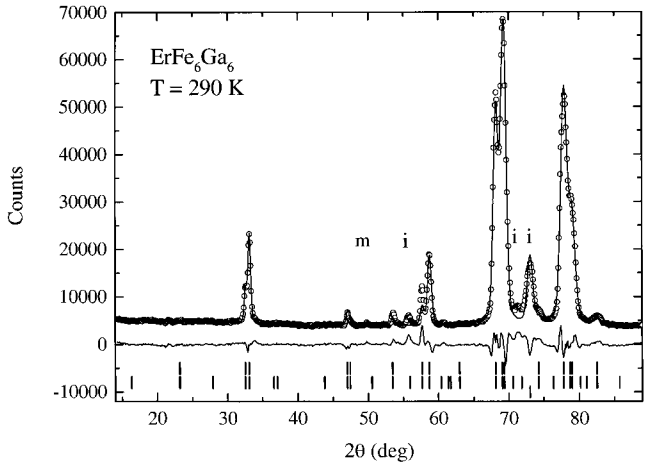

Fig. 7. Neutron-diffraction spectrum of $ErFe_6Ga_6$ recorded at 290 K. The full line through the symbols represents the best fit and the full line at the bottom represents the difference between the experimental data and the fit. The positions of α-Fe Bragg peaks and the magnetic and structural Bragg reflections of $ErFe_6Ga_6$ are marked in the first, second and the third row from the bottom. Structural and magnetic impurity peaks are denoted by "i" and "m" respectively.

the tetragonal axis. The best fit led to the same type of magnetic structure as at 2 K with moments oriented perpendicular to the tetragonal axis. The refined magnetic moments are $\mu_{Er} = 1.0$ (4) μ_B, $\mu_{Fe}8(j) = 1.9$ (5) μ_B and $\mu_{Fe}8(f) = 1.2$ (2) μ_B. During the refinement we have observed that Fe magnetic moments are strongly correlated with the overall temperature factor. Together with the fact that Er and Fe 8(f) moments tend to be strongly correlated suggests that these values should be taken with caution. The best fit, together with the measured profile, is shown in Figure 7 and the numerical results are summarized in Table 4.

4 Discussion and conclusions

The refined Er magnetic moments at 2 K are reduced by 6% with respect to their free-ion values $g_J J = 9$ μ_B ($g_J = 6/5$, $J = 15/2$). This is most likely due to crystal-field interactions which are, at low temperatures, the most important source of magnetocrystalline anisotropy. The crystal-field Hamiltonian describes the magnetocrystalline anisotropy expansion of Stevens operators multiplied by crystal-field parameters. Under assumption of a rigid coupling between Er and Fe moments, this concept can be related to phenomenological anisotropy constants $K_i(T)$, $i = 1, 2, 3, \ldots$, which are used as parameters in the expansion of the free energy $E(T)$ [13]. For the case of tetragonal symmetry (neglecting in-plane anisotropy) it can be expressed as $E(T) = K_1 \sin^2\varphi + K_2 \sin^4\varphi + K_3 \sin^6\varphi$, with φ being the angle between the magnetic moments and the tetragonal axis. If the sum of the $K_i(T)$, $i = 1, 2, 3$, is large and negative, the planar ordering is favored. In the case of $ErFe_6Ga_6$, we found planar ordering in the low-temperature ferrimagnetic phase, suggesting a large negative value of the sum of $K_i(T)$, $i = 1, 2, 3$.

Table 4. Crystallographic and magnetic-structure parameters of $ErFe_6Ga_6$ determined at 290 K.

Space group:		I_4/mmm	Neutrons $T = 290$ K (ferrimagnetic)	
Atom	Site	Pos. parameters	Occupation	Moment
Er	2(a)	000	1.00 (f)	1.04 (44)
Fe	8(f)	1/4, 1/4, 1/4	1.00 (f)	1.21 (21)
Fe	8(j)	0.2769 (8), 1/2, 0	0.50 (f)	1.86 (46)
Ga	8(j)	0.2769 (8), 1/2, 0	0.50 (f)	0
Ga	8(i)	0.3397 (8), 0, 0	1.00 (f)	0
$B_{ov} = 0.6$ (1) Å^2				
Lattice parameters:		$a = 857.664$ (129) pm	$c = 506.161$ (77) pm	
R factors:	$R_p = 4.74\%$	$R_{wp} = 6.37\%$	$R_B = 4.03\%$	$R_M = 4.89\%$

In the room-temperature ferromagnetic phase, the magnetic order was also found to be of the easy-plane type. We are planning to perform a more rigorous quantitative analysis of here presented data together with high-field magnetization measurements leading to crystal-field parameters of $ErFe_6Ga_6$ in the near future.

It is worth to compare the results obtained by means of magnetic measurements and neutron diffraction. Magnetic measurements suggest that Er and Fe moments order antiparallel to each other. Neutron diffraction fully supports this conclusion. Co-linear magnetic structure with Er and Fe moments aligned in opposite directions has been found at 2 and 290 K. However, it is hard to conclude whether both magnetic sublattices order below the same temperature of 509 K or whether only Fe moments order at high temperatures. An estimate based on extrapolation of temperature dependence of magnetic moments leads to a value of about 350 K below which both Er and Fe moments should be ordered.

Analysis of the neutron-diffraction pattern obtained at 2 K leads to magnetic moments that are in relatively good agreement with the magnetic-measurement results. From magnetic measurements it follows that Er amounts to about 7.0 μ_B and average Fe moment to 1.6 μ_B. Diffraction experiment gave us 8.5 μ_B and 1.8 μ_B, respectively. The agreement at 290 K is also reasonable. In this case, values of 0.5 μ_B/Er and 1.3 μ_B/Fe from magnetic measurements and 1.0 μ_B/Er and 1.4 μ_B/Fe from diffraction experiment have been obtained, respectively. There are few possibilities to explain the small disagreement between magnetic-moment values obtained in both experiments. One rests with the fact that our sample contains α-Fe as a secondary phase, making determination of magnetic-moment values from magnetization measurements difficult. In general, it yields Er moments that are underestimated. Second is based on the fact that certain fitted parameters, namely Fe moments at 8(f) sites on one side and Er moments and the temperature factor on the other, are strongly correlated. The discrepancy could also possibly be explained by assuming a strong reduction due to symmetry of the Fe magnetic moments at the 8(f) sites in zero magnetic field. An applied field would stabilize these magnetic moments. To discriminate between these possibilities one would need to examine a single crystal of $ErFe_6Ga_6$ in magnetic fields.

In conclusion, we have measured $ErFe_6Ga_6$ by means of magnetic and by neutron powder diffraction measurements. In spite of spurious phases that were present in our sample we were able to determine basic magnetic properties and magnetic structure of this compound between 2 and $T_C = 509$ K. The magnetic structure of $ErFe_6Ga_6$ is co-linear with Er moments antiparallel to Fe moments and perpendicular to the tetragonal axis. The type of magnetic structure does not change in the whole temperature range.

Authors would like to thank Dr. J.C.P Klaasse for his assistance with the use of the Faraday balance. This work has been supported by the Stichting voor Fundamenteel Onderzoek der Materie (FOM).

References

1. W. Suski, in *Handbook on the Physics and Chemistry of Rare Earths*, edited by K.A. Gschneidner Jr., L. Eyring (Elsevier Science, Amsterdam, 1996), Vol. 22, Chap. 149, p. 143.
2. I.A. Griniv, O.I. Golovanets, R.V. Labunova, Yu.N. Grin, Ya.P. Yarmoluk, Dopov. Akad. Nauk Ukr. RSR Ser. A **1**, 74 (1983).
3. E. Burzo, M. Valeanu, N. Plugaru, Solid State Commun. **83**, 159 (1992).
4. D.P. Middleton, K.H.J. Buschow, J. Magn. Magn. Mater. **157/158**, 385 (1996).
5. F. Weitzer, K. Hiebl, P. Rogl, Yu.N. Grin, J. Appl. Phys. **68**, 3512 (1990).
6. H.M. Rietveld, J. Appl. Cryst. **2**, 65 (1969).
7. T. Roisnel, J. Rodriguez-Carvajal, WinPLOTR (beta version - March 99), unpublished.
8. V.F. Sears, Neutron News **3**, 26 (1992).
9. G.F. Dionne, J. Appl. Phys. **40**, 1839 (1969)
10. M. Melamud, L.H. Bennett, R.E. Watson, J. Appl. Phys. **61**, 4246 (1987).
11. O. Moze, K.H.J. Buschow, Z. Phys. B **101**, 521 (1996).
12. J. Schweitzer, in *Neutron and synchrotron radiation for condensed matter studies, Vol. II - Applications to solid state physics and chemistry*, edited by J. Baruchel, J.L. Hodeau, M.S. Lehmann, J.R. Regnard, C. Schlenker (Springer-Verlag, Berlin, 1994), Chap. 5, p. 107.
13. M.T. Hutchings, Solid State Phys. **16**, 227 (1964).